ACS APPLIED MATERIALS & INTERFACES

Research Article

www.acsami.org

Healable and Optically Transparent Polymeric Films Capable of Being Erased on Demand

Yan Wang, Tianqi Li, Siheng Li, Ruibing Guo, and Junqi Sun*

State Key Laboratory of Supramolecular Structure and Materials, International Joint Research Laboratory of Nano-Micro Architecture Chemistry (NMAC), College of Chemistry, Jilin University, Changchun 130012, People's Republic of China

Supporting Information

ABSTRACT: Different from living organisms, artificial materials can only undergo a limited number of damage/healing processes and cannot heal severe damage. As an alternative to solve this problem, we report in this study the fabrication of erasable, optically transparent and healable films by exponential layer-by-layer assembly of poly(acrylic acid) (PAA) and poly(ethylene oxide) (PEO). The hydrogen-bonded PAA/PEO films are highly transparent, capable of conveniently healing damages and being erased under external stimuli. The PAA/PEO films can heal damages such as scratches and deep cuts for multiple times in the same location by exposure to pH 2.5 water or humid N_2 flow. The healability of the PAA/PEO films originates from the reversibility of the hydrogen bonding interaction between PAA and PEO, and the tendency of films to flow upon adsorption of water. When the damage exceeds the capability of the films to repair, the damaged films can be conveniently erased from substrates to facilitate the replacement of the damaged films with new ones. The combination of healability and erasibility provides a new way to the design of transparent films with enhanced reliability and extended service life.

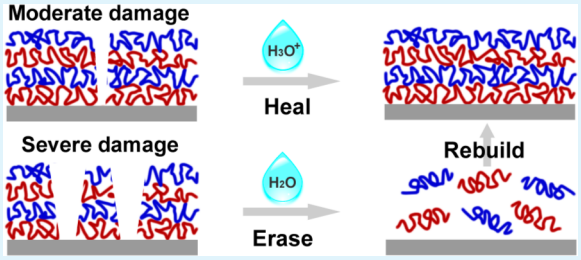

KEYWORDS: *erasable films, layer-by-layer, materials science, polymeric films, self-healing*

INTRODUCTION

The ability of living organisms to repair damage increases their chance of survival and extends their lifetime.[1−4] For example, human skin can heal wounds to reduce the risk of death due to bacterial and fungal infection. In the beginning, injury triggers the inflammatory response of skin. Then, with the help of replenishment of materials and energy from the circulatory systems and adjacent tissues, cells around the injury area can proliferate and finally cover the denuded wound surface with newly regenerated skin.[2,3] Inspired by the fascinating features of self-healing ability of living organisms, elegant artificial self-healing/healable materials have been successfully fabricated, which not only reduces the maintenance costs but also significantly prolongs the lifetime and improves the reliability of the artificial materials.[1,5−19] Different from living organisms that can continuously obtain nutrients from environments to promote wound healing, most of the artificial materials can only undergo a limited number of damage/healing processes and cannot heal severe damage.[5,13−17] This is because of the following: (i) the depletion of the raw materials because no external supply of raw materials is available after repeated damage/healing processes;[5,15,16] (ii) the lack of efficient methods to transport sufficient healing agents through a long distance to the damaged region both in extrinsic and intrinsic self-healing materials.[13,17] This problem, which has troubled scientists for a long time, becomes more obvious in self-healing/healable thin films than in self-healing/healable bulk materials.[15,17,18] Close-then-heal (CTH) systems were developed by Li and co-workers to heal wide-opened cracks in millimeter scale. The CHT system heals large damage by first forcing the damaged areas to come into contact and then initiating the healing process. However, this method is not suitable for self-healing/healable films deposited on solid substrates.[20−22]

Among various functional films, healable, optically transparent films are highly important but their fabrication remains a huge challenge.[1,15,23] Optically transparent films can find applications as protective and functional layers for various optical and display devices.[15,23−27] Scratches on transparent films change the way of light transmission and even cause severe light scattering. Such scratches on transparent films have to be healed to restore their original optical functions for further applications. Otherwise, the healable optical films with irreparable scratches need to be replaced with new films after being completely removed from the targeted substrates or devices. Therefore, erasibility and healability are highly required to be integrated into optically transparent films to enable convenient healing of damage and removal of the films from the underlying substrates when the damage exceeds their capability to repair.

Previous studies show that the fabrication of healable, transparent films by using the capsule-based extrinsic method is

Received: April 13, 2015
Accepted: June 4, 2015
Published: June 4, 2015

DOI: 10.1021/acsami.5b03179
ACS Appl. Mater. Interfaces 2015, 7, 13597−13603

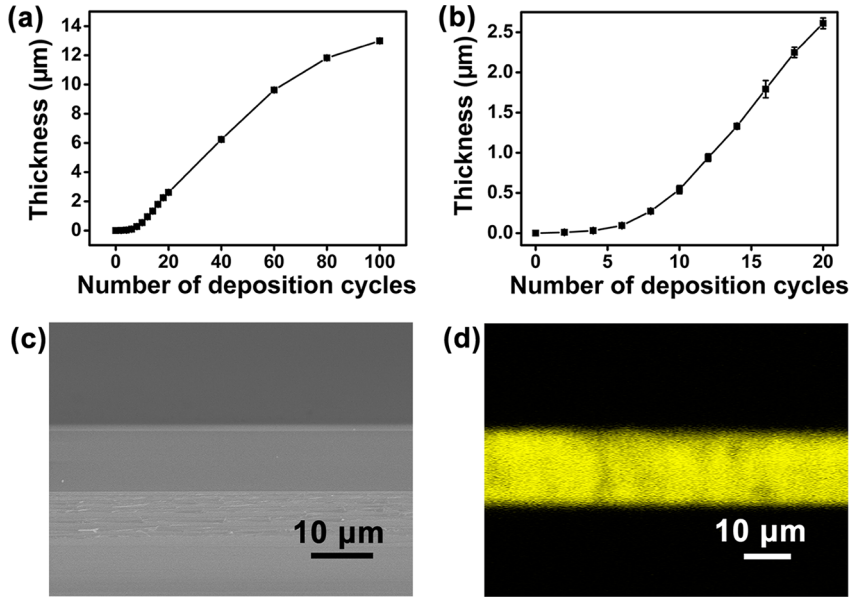

Figure 1. (a, b) Thickness of (PAA/PEO)*n films as a function of the number of film deposition cycles. (c, d) Cross-sectional (c) SEM and (d)CLSM images of a (PAA/PEO)*100/PAA-LYC film.

technically difficult because the capsules, which contain healing agents and usually have sizes of several to several tens of micrometers, strongly scatter visible light.[1,23,27] The intrinsic healable method, which heals damage through the inherent reversibility of noncovalent interactions[15,18] and dynamic covalent bonds,[6,28,29] is suitable for fabricating optically transparent healable films because no externally added healing agent is required. The layer-by-layer (LbL) assembly method, which involves alternate deposition of species with noncovalent interactions,[30−34] has been successfully employed to fabricate water-enabled healable polymeric films.[15,17,18,35,36] In our previous work, we demonstrated the fabrication of optically transparent antibacterial films capable of restoring transparency caused by scratches by LbL assembly of branched polyethylenimine (bPEI) and poly(acrylic acid) (PAA) and postloading of the bPEI/PAA films with antibacterial agent triclosan.[15] The triclosan-loaded transparent antibacterial bPEI/PAA films can heal shallow scratches of several micrometers wide but fail to heal scratches which are penetrated to the underlying substrates. The diversity of driving forces for LbL-assemble films provides opportunity for the design of healable transparent polymeric films which can be completely decomposed under external stimuli. In this study, as a proof-of-concept, we report that LbL assembly of poly(acrylic acid) (PAA) and poly(ethylene oxide) (PEO) produces hydrogen-bonded transparent PAA/PEO films that can conveniently heal damages and are capable of being erased from substrates on demand. Scratches penetrating to substrate surface can be healed by immersing the films in acidic water. Importantly, when the scratches exceed the capability of the films to heal, the damaged films can be completely erased from substrates. The combination of erasable and healable properties will provide a new pattern to the design of novel healable film materials.

EXPERIMENTAL SECTION

Materials. Poly(diallyldimethylammonium chloride) (PDDA, M_w ca. 100 000−200 000), PAA (M_w ca. 100 000) and PEO (M_w ca. 100 000) were purchased from Sigma-Aldrich. Lucifer yellow cadaverine (LYC) was purchased from Invitrogen. All chemicals were used without further purification. Deionized water was used for all film fabrication. LYC-labeled PAA (PAA-LYC) was synthesized according to a literature method.[17] In the reaction vessels, the fed molar ratio of LYC molecules and carboxylate group in PAA was 1:100. Aqueous PEO solution was heated to 60 °C for 2 h and then cooled to room temperature to ensure its complete dissolution. The pH of the PAA and PEO dipping solutions was adjusted with 10 M HCl.

Fabrication of PAA/PEO Films. A newly cleaned substrate (quartz, glass or silicon wafers) was first immersed in an aqueous PDDA solution (1 mg mL^{-1}) for 20 min to obtain a cationic ammonium-terminated surface. The PDDA modified-substrate was then immersed into aqueous PAA solution (2 mg mL^{-1}, pH 2.5) for 5 min to obtain a layer of PAA film, followed by rinsing in three water baths (pH 2.5) for 1 min each to remove the physically absorbed PAA. The substrate was subsequently immersed into aqueous PEO solution (2 mg mL^{-1}, pH 2.5) for 5 min to obtain a layer of PEO film, followed by rinsing in three water baths (pH 2.5) for 1 min each. The deposition of PAA and PEO was repeated until the desired number of deposition cycles was obtained. No drying steps were used in the film deposition procedure until it was in the last layer.

Film Characterization. Scanning electron microscopy (SEM) images were obtained on a JEOL JSM 6700F field emission scanning electron microscope. Film thicknesses were measured by a Veeco Dektak 150 profilometer with 3 mg stylus force. The diffusion of LYC-labeled PAA in PAA/PEO multilayer films was viewed with an Olympus FV1000 confocal laser scanning microscope. Digital camera images were captured using a Canon camera (Power Shot S3 IS). Optical micrographs were taken with an Olympus BX-51 optical microscope. UV−vis transmission spectra were recorded with a Shimadzu UV-2550 spectrophotometer. Atomic force microscopy (AFM) images were taken on a commercial instrument (Veeco Company Nanoscope IV) in tapping mode under ambient environment. An Agilent Nano Indenter G200 with the continuous stiffness measurement (CSM) method and XP-style actuator was used to measure the mechanical properties of the films. Modulus of the films in air was measured with a Berkovich diamond indenter with a relative humidity (RH) of ∼20% at 30 °C. Storage modulus of the films in pH 2.5 water was measured with a flat-ended cylindrical punch made of diamond by the "G-Series XP CSM flat punch complex modulus" method. The detailed measurements were made according to our previous publication.[15]

DOI: 10.1021/acsami.5b03179
ACS Appl. Mater. Interfaces 2015, 7, 13597−13603

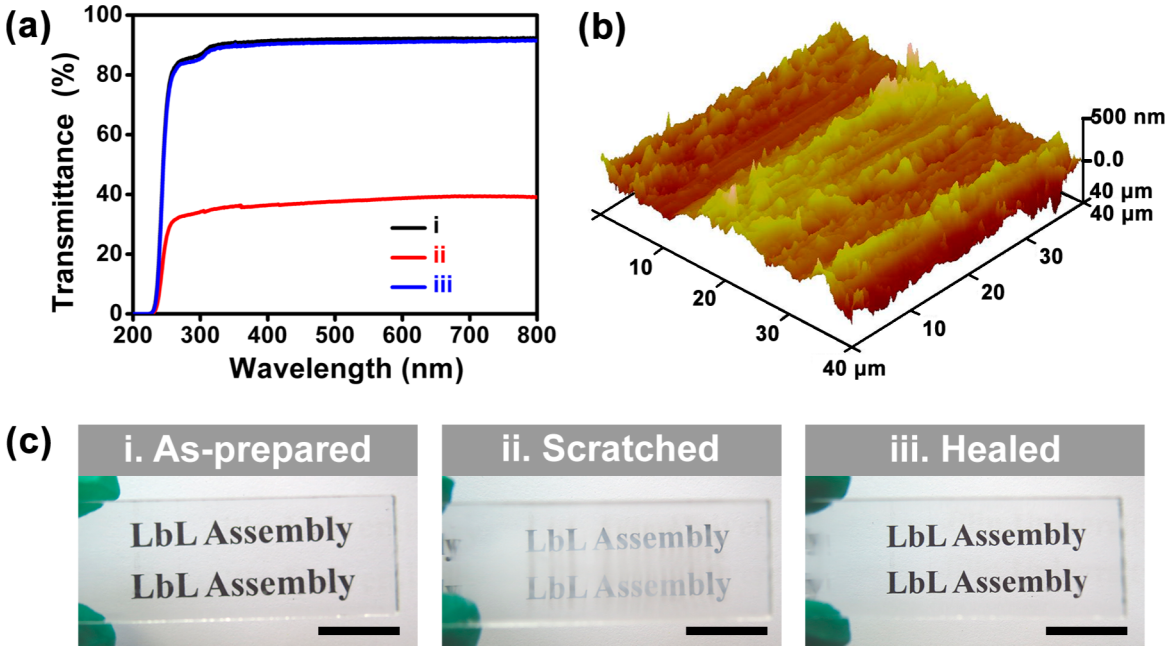

Figure 2. (a) UV−vis transmission spectra of a (PAA/PEO)*100 film. (i) As-prepared film; (ii) film in (i) after being scratched with sandpaper; (iii) film in (ii) after healing in pH 2.5 water for 30 min. (b) AFM image of a scratched (PAA/PEO)*100 film. (c) Digital images of a (PAA/PEO)*100 film on a quartz substrate that heals scratches. (i) As-prepared film; (ii) film in (i) after being scratched with sandpaper; (iii) film in (ii) after healing in pH 2.5 water for 30 min. The scale bar is 1 cm.

RESULTS AND DISCUSSION

LbL Exponential Growth of PAA/PEO Films. PAA is a kind of weak polyelectrolyte, whose ionization in aqueous solution is pH-dependent.[37,38] A previous study showed that even with ∼5% ionization degree of carboxylate groups, the negatively charged groups on PAA can significantly prevent its LbL assembly with PEO via hydrogen bonding interaction as the driving force.[38] To enable the alternate deposition of PAA and PEO via hydrogen bonding interaction, we set the pH of the PAA and PEO dipping solutions and the rinsing water at 2.5. At such a low solution pH, the ionization of PAA was largely suppressed.[37−40] The newly cleaned substrates (quartz and silicon wafers) were predeposited with a layer of PDDA and then the alternate deposition of PAA and PEO was conducted to produce hydrogen-bonded (PAA/PEO)*n films (where n refers to the number of film deposition cycles), in which carboxylic groups of PAA form hydrogen bonds with ether oxygens of PEO. The thickness of the (PAA/PEO)*n films with different deposition cycles were determined by a profilometer (Figure 1a, b). For the initial 20 deposition cycles, the film thickness exhibits a typically exponential growth behavior. After 20 deposition cycles, a nearly linear deposition of PAA/PEO films is observed, with an average increment of ∼130 nm for one cycle of PAA/PEO film. The slight deviation of linear deposition after the 60th deposition cycle is caused by the gradually decreased concentrations of the dipping solutions. The thickness of the (PAA/PEO)*100 films reaches 12.9 ± 0.5 μm. Cross-sectional SEM image in Figure 1c discloses a conformal, compact and flat (PAA/PEO)*100/PAA-LYC film on silicon substrate with a constant thickness of 13.0 ± 0.3 μm. This value is consistent with that measured by a profilometer. PAA-LYC was deposited as the outmost layer of a (PAA/PEO)*100 film and the diffusion of PAA-LYC into the film was characterized by confocal laser scanning microscopy (CLSM). CLSM image in Figure 1d shows that PAA-LYC can diffuse throughout the entire film. According to previous studies on exponentially grown LbL-assembled polyelectrolyte films,[41−44] the exponential growth of the PAA/PEO can be ascribed to the "in-and-out" diffusion of PAA during the PAA/PEO film fabrication. The "in-diffusion" of PAA leads to an excessive deposition of PAA in aqueous PAA dipping solution, which in turn results in an excessive deposition of PEO in aqueous PEO solution because of the "out-diffusion" of PAA. In this way, the thickness of the PAA/PEO films increases exponentially. With increasing number of film deposition cycles, the amount of the diffused PAA gradually reaches constant and a linear growth of PAA/PEO films is then obtained.

Restoring Transparency of PAA/PEO Films. The (PAA/PEO)*100 films are colorless and transparent with an extremely smooth surface. AFM image shows that the (PAA/PEO)*100 film with a measured area of 40 × 40 μm has a root-mean-square (RMS) roughness of ∼5 nm (see the Supporting Information, Figure S1). As shown in Figure 2a (curve (i)), in the whole visible light region, the (PAA/PEO)*100 film is highly transparent, with its transmittance at 550 nm being ∼92%. The transparency of the (PAA/PEO)*100 film on quartz substrate significantly decreased to ∼40% at 550 nm when the film was repeatedly scratched with a 2000-grit sandpaper (Figure 2a, curve (ii)). AFM image in Figure 2b shows that the repeatedly scratched (PAA/PEO)*100 film is full of grooves of 4.3 ± 1.0 μm wide and 1.3 ± 0.4 μm deep, which strongly scatter visible light. After immersing the scratched (PAA/PEO)*100 film in pH 2.5 water for 30 min, the original transparency of the film is fully restored, as indicated in curve iii of Figure 2a. The damage-healing process of the (PAA/PEO)*100 film on a quartz substrate is depicted in Figure 2c. The scratches on the (PAA/PEO)*100 film are clearly seen, which lead to blur of the underneath words because of the strong visible light scattering. The transparency of the healed (PAA/PEO)*100 film in acidic water shows no

DOI: 10.1021/acsami.5b03179
ACS Appl. Mater. Interfaces 2015, 7, 13597−13603

difference with that of the as-prepared film, with the underneath words being clearly seen again.

The time-dependent healing process of the (PAA/PEO)*100 film was characterized by optical microscopy. As shown in Figure 3a, the surface of the scratched (PAA/PEO)*100 film is

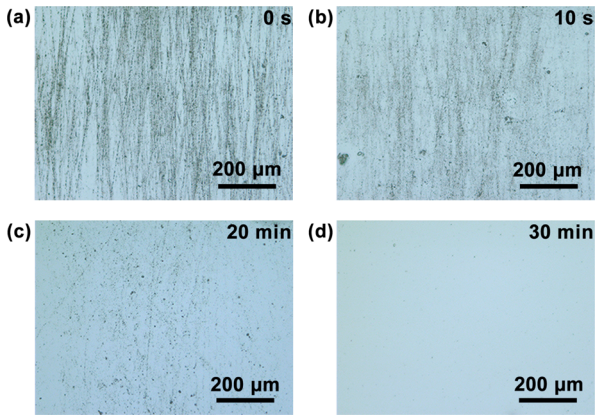

Figure 3. (a–d) Visual observation of the healing process of a (PAA/PEO)*100 film. (a) Scratched film; (b–d) scratched film after being immersed in pH 2.5 water for (b) 10 s, (c) 20 min, and (d) 30 min.

full of scratches. After being immersed in pH 2.5 water for 10 s, the density of scratches decreases, indicating that the healing of scratches takes place (Figure 3b). The density of scratches decreases obviously after a 20 min immersion in pH 2.5 water (Figure 3c). However, the complete healing of the scratches takes about 30 min (Figure 3d). The sandpaper-scratched (PAA/PEO)*100 film undergoes five cycles of damage/healing processes and their transmittance at 550 nm was monitored by UV–vis transmission spectroscopy. As shown in Figure 4a, the transmittance at 550 nm of the repeatedly scratched (PAA/PEO)*100 film is ~40% because the scratches largely reduces the flux of light transmission. The transmittance of the healed film at 550 nm reaches ~92% after each healing process, confirming that the transparency of the film is successfully restored even after 5 damage-healing cycles. Therefore, the optically transparent (PAA/PEO)*100 films can heal scratches and restore transparency for multiple times in a given area. The fine restoration of the film transparency originates from the disappearance of the scratches, which is confirmed by the RMS roughness changes of the film during multiple damage/healing processes. As indicated in Figure 4b, RMS roughness of the healed (PAA/PEO)*100 film restores to its original value after each healing process. Moreover, the optical transparency of the (PAA/PEO)*100 films can be also restored by exposing the scratched films to a humid N_2 flow, which produces an environment with a RH of ~70%. With humid N_2 flow, healing of scratches made by sandpaper can be completed within 2 min. After 5 cycles of damage with sandpaper and healing with a humid N_2 flow, the transmittance of the (PAA/PEO)*100 film at 550 nm reaches ~89% (see the Supporting Information, Figure S2).

Restoring Structural Integrity of PAA/PEO Films. The (PAA/PEO)*100 films can heal not only tiny and shallow scratches to restore the transparency but also wide and deep cuts to rebuild the structural integrity. A cut of ~11 μm wide that penetrates to the underlying substrate was made on the (PAA/PEO)*100 film by a scalpel (Figure 5a). SEM image

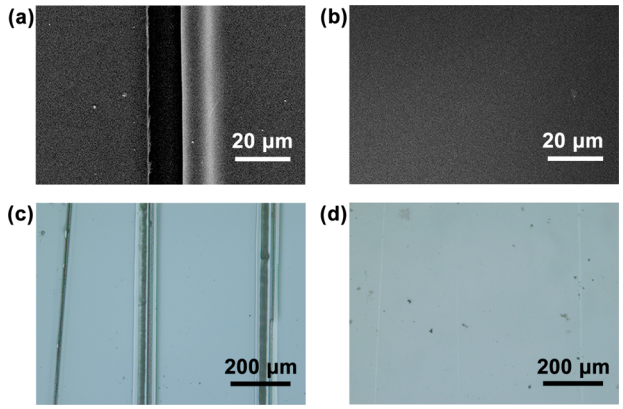

Figure 5. (a, b) SEM images of a (PAA/PEO)*100 film with a cut of ~11 μm wide (a) before and (b) after being healed. (c, d) Optical microscope images of a (PAA/PEO)*100 film with 3 cuts (c) before and (d) after being healed.

indicates that the cut can be totally healed by immersing the damaged film in pH 2.5 water for 30 min (Figure 5b). Three adjacent cuts were made within a width range of ~0.9 mm on the (PAA/PEO)*100 film, with their width ranging from ~4.7 μm to ~9.4 μm (Figure 5c). Optical microscope image in Figure 5d shows that these three cuts are finely healed in pH 2.5 water. Please note that the SEM image of the healed (PAA/PEO)*100 film in Figure 5b was taken under a vacuum condition. Therefore, drying cannot lead to recrack of the healed (PAA/PEO)*100 films. Different from our previously reported healable and transparent bPEI/PAA films, which can only heal shallow scratches made by sandpaper, the PAA/PEO films have a stronger ability to heal larger and deeper cuts made by a scalpel. The (PAA/PEO)*100 film can heal a cut with a maximum width of ~36 μm when the healing time in pH 2.5 water is prolonged to 24 h (see the Supporting Information,

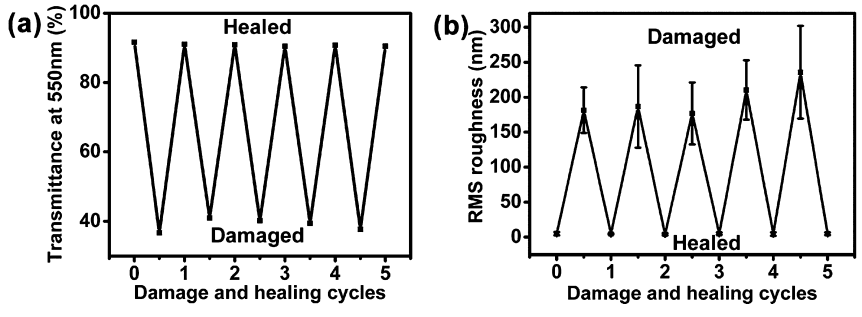

Figure 4. Changes of transmittance at 550 nm (a) and RMS roughness (b) of a (PAA/PEO)*100 film during five damage/healing cycles.

DOI: 10.1021/acsami.5b03179
ACS Appl. Mater. Interfaces 2015, 7, 13597–13603

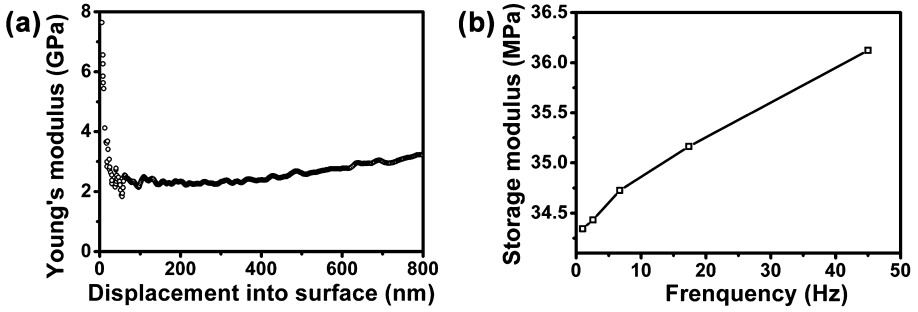

Figure 6. (a) Young's modulus of a (PAA/PEO)*100 film as a function of penetration depth at 30 °C with a RH of 20%. (b) Storage modulus of a (PAA/PEO)*100 film in pH 2.5 water as a function of frequency.

Figure S3). Moreover, the (PAA/PEO)*100 film can perform repeated healing of deep cut in the same area. Cuts of ∼11 μm in width are hardly seen after the cutting-healing process has been repeated for 5 times on a (PAA/PEO)*100 film (see the Supporting Information, Figure S4). The LbL assembly of optically transparent and healable (PAA/PEO)*n films can be further accelerated by increasing concentrations of PAA and PEO dipping solutions to 3 mg mL^{-1} and decreasing water rinsing time to 1 min/layer with one water rinsing bath being used (see the Supporting Information, Figure S5).

To understand the healing mechanism of the PAA/PEO films, we measured their mechanical properties under dry conditions and in acidic water by nanoindentation. The CSM technique with a Berkovich diamond indenter with a radius ≤20 nm was used to measure Young's modulus of (PAA/PEO)*100 films in air with ∼20% RH at 30 °C.[15] Figure 6a shows the Young's modulus of the (PAA/PEO)*100 film as a function of indenter displacement. The modulus is large and decreases sharply in the initial stage (<100 nm), which might imply that the outmost layer of the film is harder than the interior film. Then the modulus reaches a plateau in the displacement region of 150−250 nm. The average value in this plateau region is the "real" Young's modulus of the (PAA/PEO)*100 film, which is 2.1 ± 0.2 GPa. The modulus gradually increases over a displacement of ∼250 nm, in which the influence of substrate on the measured modulus becomes obvious. A flat-ended cylindrical punch made of diamond with a diameter of 108.5 μm was used to measure storage modulus of the (PAA/PEO)*100 films in pH 2.5 water by the "G-Series XP CSM Flat Punch Complex Modulus" method.[15] Figure 6b displays the storage modulus of the film increases with increasing frequency. Because healing of the (PAA/PEO)*100 films was conducted in undisturbed water, storage modulus under a low frequency of 1 Hz, which is 32.7 ± 2.0 MPa, was chosen to analyze the mechanical property of the films during healing in pH 2.5 water. A significant decrease of modulus of the (PAA/PEO)*100 films occurs when the films in dry conditions was transferred into pH 2.5 water, meaning that the films in water become soft and flowable. This was supported by the swelling of the (PAA/PEO)*100 films when immersing the films in pH 2.5 water. The saturation water absorption in (PAA/PEO)*100 film is achieved within 1 min, which leads to a film thickness increase of ∼275% (see the Supporting Information, Figure S6). When immersed in acidic water, ether oxygens can form hydrogen bonds with water molecules, which weaken the hydrogen bonds between PAA and PEO (see the Supporting Information, Figure S7). The adsorbed water in PAA/PEO films can also act as plasticizers to facilitate the mobility of PAA and PEO polymer chains. Therefore, the storage modulus of the PAA/PEO films decreases largely and the films become flowable when they are immersed in water. The migration of PAA and PEO fills the scratches and cuts, where they reform hydrogen bonding interactions. Therefore, the reversibility of hydrogen bonds and the facilitated migration of PAA and PEO by water molecules enable healing of the structural integrity and the optical transparency of the (PAA/PEO)*100 films.

Erasing of PAA/PEO Films under Severe Damage. The healable (PAA/PEO)*100 films with severe damages cannot be healed because of the lack of polymers that can migrate to the damaged region. As shown in Figure 7a, three cuts with width

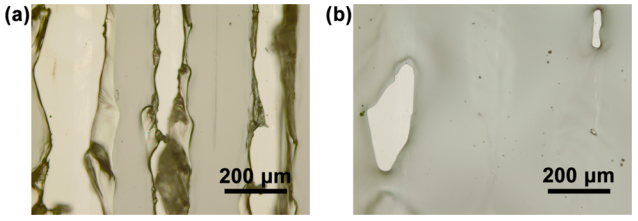

Figure 7. Optical microscope images of a (PAA/PEO)*100 with severe cuts (a) before and (b) after being healed in pH 2.5 water for 24 h.

ranging from ∼49 μm to ∼204 μm were made on a (PAA/PEO)*100 film within a width range of ∼0.9 mm. The damaged film failed to completely heal the cuts even immersing the film in pH 2.5 water for 24 h (Figure 7b). The (PAA/PEO)*100 film with irreparable damage requires to be removed from the underlying substrate to facilitate redeposition of PAA/PEO films. The hydrogen bonding interaction between PAA and PEO is pH sensitive and can be stable only in acidic water.[38] When the (PAA/PEO)*100 films were immersed in deionized water (pH 6.8) at room temperature, gradual decomposition of the films was observed (Figure 8). The (PAA/PEO)*100 films completely decomposed within 4 h immersion in deionized water. In deionized water, PAA is highly deprotonated and becomes negatively charged, which breaks its hydrogen bonding interaction with PEO. Previous study indicates that ∼5% ionization of PAA in pH 3.5 aqueous solution can produce sufficient negative charge to prohibit complexation with PEO.[38] The decomposition of the PAA/PEO films is pH dependent, with a quicker decomposition in water of higher pH value.[37−39] The decomposition of the PAA/PEO films occurs when pH of water is higher than 3.0. Therefore, healing of the damaged PAA/PEO films is performed by immersing the films in water with a pH lower than 3.0. The easily erasing of the healable and transparent

DOI: 10.1021/acsami.5b03179
ACS Appl. Mater. Interfaces 2015, 7, 13597−13603

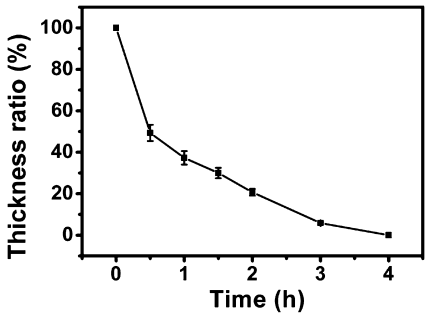

Figure 8. Erasing process of a (PAA/PEO)*100 film as a function of the immersion time in water. Error bars represent the average standard deviation of measured thickness values from three different locations on the film.

PAA/PEO films from substrates means that the films can be conveniently replaced with new ones when the damage is beyond the capability of the films to repair.

CONCLUSIONS

We have demonstrated the fabrication of erasable, optically transparent and healable PAA/PEO films by exponential LbL assembly technique. The transparent PAA/PEO films can repeatedly heal damages such as scratches and deep cuts in the same location by exposure of the films to pH 2.5 water or humid N_2 flow. Moreover, the PAA/PEO films can be conveniently erased from substrates through direct film dissolution when the damages are beyond the capability of the film to heal. The reversibility and dynamic nature of the hydrogen bonds between PAA and PEO endow the PAA/PEO films with satisfied healability and erasibility. The deposition of LbL-assembled PAA/PEO is independent of the morphology and type of substrates. Therefore, the transparent, erasable and healable PAA/PEO films can find potential applications on various surfaces as optical functional films. Moreover, other kinds of transparent, erasable and healable films can be fabricated following the designed principle provided in this work. The combination of healability and erasibility provides not only a new way to the design of transparent films with enhanced reliability and extended service life, but also an alternative method to solve the problem that artificial materials can only undergo a limited number of damage/healing processes and cannot heal severe damage.

ASSOCIATED CONTENT

Supporting Information

AFM image of the as-prepared (PAA/PEO)*100 film, multiple healing of transparency of a (PAA/PEO)*100 film by exposure to humid N_2 flow, and optical microscope images of the (PAA/PEO)*100 films with cuts of different width before and after healing. The Supporting Information is available free of charge on the ACS Publications website at DOI: 10.1021/acsami.5b03179.

AUTHOR INFORMATION

Corresponding Author

*E-mail sun_junqi@jlu.edu.cn.

Author Contributions

The manuscript was written through contributions of all authors. All authors have given approval to the final version of the manuscript.

Funding

This work was supported by the National Basic Research Program (2013CB834503) and the National Natural Science Foundation of China (NSFC Grants 21225419 and 21221063).

Notes

The authors declare no competing financial interest.

ABBREVIATIONS

PAA, poly(acrylic acid)
PEO, poly(ethylene oxide)
LbL, layer-by-layer
PDDA, poly(diallyldimethylammonium chloride)
LYC, lucifer yellow cadaverine

REFERENCES

(1) Blaiszik, B. J.; Kramer, S. L. B.; Olugebefola, S. C.; Moore, J. S.; Sottos, N. R.; White, S. R. Self-Healing Polymers and Composites. *Annu. Rev. Mater. Res.* **2010**, *40*, 179−211.
(2) Martin, P. Wound Healing–Aiming for Perfect Skin Regeneration. *Science* **1997**, *276*, 75−81.
(3) Singer, A. J.; Clark, R. A. F. Cutaneous Wound Healing. *N. Engl. J. Med.* **1999**, *341*, 738−746.
(4) Odland, G.; Ross, R. Human Wound Repair. *J. Cell Biol.* **1968**, *39*, 135−168.
(5) White, S. R.; Sottos, N. R.; Geubelle, P. H.; Moore, J. S.; Kessler, M. R.; Sriram, S. R.; Brown, E. N.; Viswanathan, S. Autonomic Healing of Polymer Composites. *Nature* **2001**, *409*, 794−797.
(6) Deng, G.; Tang, C.; Li, F.; Jiang, H.; Chen, Y. Covalent Cross-Linked Polymer Gels with Reversible Sol-Gel Transition and Self-Healing Properties. *Macromolecules* **2010**, *43*, 1191−1194.
(7) Cordier, P.; Tournilhac, F.; Soulié-Ziakovic, C.; Leibler, L. Self-Healing and Thermoreversible Rubber from Supramolecular Assembly. *Nature* **2008**, *451*, 977−980.
(8) Chen, Y.; Kushner, A. M.; Williams, G. A.; Guan, Z. Multiphase Design of Autonomic Self-Healing Thermoplastic Elastomers. *Nat. Chem.* **2012**, *4*, 467−472.
(9) Andreeva, D. V.; Fix, D.; Möhwald, H.; Shchukin, D. G. Self-Healing Anticorrosion Coatings Based on pH-Sensitive Polyelectrolyte/Inhibitor Sandwichlike Nanostructures. *Adv. Mater.* **2008**, *20*, 2789−2794.
(10) Li, Y.; Chen, S.; Wu, M.; Sun, J. Rapid and Efficient Multiple Healing of Flexible Conductive Films by Near-Infrared Light Irradiation. *ACS Appl. Mater. Interfaces* **2014**, *6*, 16409−16415.
(11) Zheng, Z.; Huang, X.; Schenderlein, M.; Borisova, D.; Cao, R.; Möhwald, H.; Shchukin, D. Self-Healing and Antifouling Multifunctional Coatings Based on pH and Sulfide Ion Sensitive Nanocontainers. *Adv. Funct. Mater.* **2013**, *23*, 3307−3314.
(12) Wang, C.; Liu, N.; Allen, R.; Tok, J. B.-H.; Wu, Y.; Zhang, F.; Chen, Y.; Bao, Z. A Rapid and Efficient Self-Healing Thermo-Reversible Elastomer Crosslinked with Graphene Oxide. *Adv. Mater.* **2013**, *25*, 5785−5790.
(13) Barthel, M. J.; Rudolph, T.; Teichler, A.; Paulus, R. M.; Vitz, J.; Hoeppener, S.; Hager, M. D.; Schacher, F. H.; Schubert, U. S. Self-Healing Materials via Reversible Crosslinking of Poly(ethyleneoxide)-Block-Poly(furfuryl glycidyl ether) (PEO-b-PFGE) Block Copolymer Films. *Adv. Funct. Mater.* **2013**, *23*, 4921−4932.
(14) Peterson, A. M.; Jensen, R. E.; Palmese, G. R. Room-Temperature Healing of a Thermosetting Polymer Using the Diels-Alder Reaction. *ACS Appl. Mater. Interfaces* **2010**, *2*, 1141−1149.
(15) Wang, X.; Wang, Y.; Bi, S.; Wang, Y.; Chen, X.; Qiu, L.; Sun, J. Optically Transparent Antibacterial Films Capable of Healing Multiple Scratches. *Adv. Funct. Mater.* **2014**, *24*, 403−411.
(16) Caruso, M. M.; Blaiszik, B. J.; White, S. R.; Sottos, N. R.; Moore, J. S. Full Recovery of Fracture Toughness Using a Nontoxic Solvent-Based Self-Healing System. *Adv. Funct. Mater.* **2008**, *18*, 1898−1904.

DOI: 10.1021/acsami.5b03179
ACS Appl. Mater. Interfaces 2015, 7, 13597−13603

(17) Wang, X.; Liu, F.; Zheng, X.; Sun, J. Water-Enabled Self-Healing of Polyelectrolyte Multilayer Coatings. *Angew. Chem., Int. Ed.* **2011**, *50*, 11378−11381.
(18) South, A. B.; Lyon, L. A. Autonomic Self-Healing of Hydrogel Thin Films. *Angew. Chem., Int. Ed.* **2010**, *49*, 767−771.
(19) Hong, G.; Zhang, H.; Lin, Y.; Chen, Y.; Xu, Y.; Weng, W.; Xia, H. Mechanoresponsive Healable Metallosupramolecular Polymers. *Macromolecules* **2013**, *46*, 8649−8656.
(20) Li, G.; Uppu, N. Shape Memory Polymer Based Self-Healing Syntactic Foam: 3-D Confined Thermomechanical Characterization. *Compos. Sci. Technol.* **2010**, *70*, 1419−1427.
(21) Li, G.; Meng, H.; Hu, J. Healable Thermoset Polymer Composite Embedded with Stimuli-Responsive Fibres. *J. R. Soc. Interface* **2012**, *9*, 3279−3287.
(22) Zhang, P.; Li, G. Healing-on-Demand Composites Based on Polymer Artificial Muscle. *Polymer* **2015**, *64*, 29−38.
(23) Jackson, A. C.; Bartelt, J. A.; Braun, P. V. Transparent Self-Healing Polymers Based on Encapsulated Plasticizers in a Thermoplastic Matrix. *Adv. Funct. Mater.* **2011**, *21*, 4705−4711.
(24) Shimomura, H.; Gemici, Z.; Cohen, R. E.; Rubner, M. F. Layer-by-Layer-Assembled High-Performance Broadband Antireflection Coatings. *ACS Appl. Mater. Interfaces* **2010**, *2*, 813−820.
(25) Lee, H.; Alcaraz, M. L.; Rubner, M. F.; Cohen, R. E. Zwitter-Wettability and Antifogging Coatings with Frost-Resisting Capabilities. *ACS Nano* **2013**, *7*, 2172−2185.
(26) Li, Y.; Cui, P.; Wang, L.; Lee, H.; Lee, K.; Lee, H. Highly Bendable, Conductive, and Transparent Film by an Enhanced Adhesion of Silver Nanowires. *ACS Appl. Mater. Interfaces* **2013**, *5*, 9155−9160.
(27) Amendola, V.; Meneghetti, M. Advances in Self-Healing Optical Materials. *J. Mater. Chem.* **2012**, *22*, 24501−24508.
(28) Gong, C.; Liang, J.; Hu, W.; Niu, X.; Ma, S.; Hahn, H. T.; Pei, Q. A Healable, Semitransparent Silver Nanowire-Polymer Composite Conductor. *Adv. Mater.* **2013**, *25*, 4186−4191.
(29) Lafont, U.; Zeijl, H. V.; Zwaag, S. V. D. Influence of Cross-linkers on the Cohesive and Adhesive Self-Healing Ability of Polysulfide-Based Thermosets. *ACS Appl. Mater. Interfaces* **2012**, *4*, 6280−6288.
(30) Decher, G. Fuzzy Nanoassemblies: Toward Layered Polymeric Multicomposites. *Science* **1997**, *277*, 1232−1237.
(31) Zhang, X.; Chen, H.; Zhang, H. Layer-by-layer Assembly: from Conventional to Unconventional Methods. *Chem. Commun.* **2007**, *14*, 1395−1405.
(32) Li, Y.; Wang, X.; Sun, J. Layer-by-layer Assembly for Rapid Fabrication of Thick Polymeric Films. *Chem. Soc. Rev.* **2012**, *41*, 5998−6009.
(33) Yan, Y.; Björnmalm, M.; Caruso, F. Assembly of Layer-by-Layer Particles and Their Interactions with Biological Systems. *Chem. Mater.* **2014**, *26*, 452−460.
(34) Srivastava, S.; Kotov, N. A. Composite Layer-by-Layer (LBL) Assemblly with Inorganic Nanoparticles and Nanowires. *Acc. Chem. Res.* **2008**, *41*, 1831−1841.
(35) Li, Y.; Chen, S.; Wu, M.; Sun, J. Polyelectrolyte Multilayers Impart Healability to Highly Electrically Conductive Films. *Adv. Mater.* **2012**, *24*, 4578−4582.
(36) Dou, Y.; Zhou, A.; Pan, T.; Han, J.; Wei, M.; Evans, D. G.; Duan, X. Humidity-Triggered Self-Healing Films with Excellent Oxygen Barrier Performance. *Chem. Commun.* **2014**, *50*, 7136−7138.
(37) Sukhishvili, S. A.; Granick, S. Layered, Erasable Polymer Multilayers Formed by Hydrogen-Bonded Sequential Self-Assembly. *Macromolecules* **2002**, *35*, 301−310.
(38) DeLongchamp, D. M.; Hammond, P. T. Highly Ion Conductive Poly(ethylene oxide)-Based Solid Polymer Electrolytes from Hydrogen Bonding Layer-by-Layer Assembly. *Langmuir* **2004**, *20*, 5403−5411.
(39) Kim, B.; Park, S. W.; Hammond, P. T. Hydrogen-Bonding Layer-by-Layer Assembled Biodegradable Polymeric Micelles as Drug Delivery Vehicles from Surfaces. *ACS Nano* **2008**, *2*, 386−392.
(40) Lutkenhaus, J. L.; Hrabak, K. D.; Mcennis, K.; Hammond, P. T. Elastomeric Flexible Free-Standing Hydrogen-Bonded Nanoscale Assemblies. *J. Am. Chem. Soc.* **2005**, *127*, 17228−17234.
(41) Picart, C.; Mutterer, J.; Richert, L.; Luo, Y.; Prestwich, G. D.; Shaaf, P.; Voegel, J.-C.; Lavalle, P. Molecular Basis for the Explanation of the Exponential Growth of Polyelectrolyte Multilayers. *Proc. Natl. Acad. Sci. U.S.A.* **2002**, *99*, 12531−12535.
(42) Porcel, C.; Lavalle, P.; Ball, V.; Decher, G.; Senger, B.; Voegel, J.-C.; Schaaf, P. From Exponential to Linear Growth in Polyelectrolyte Multilayers. *Langmuir* **2006**, *22*, 4376−4383.
(43) Podsiadlo, P.; Michel, M.; Lee, J.; Verploegen, E.; Kam, N. W. S.; Ball, V.; Lee, J.; Qi, Y.; Hart, A. J.; Hammond, P. T.; Kotov, N. A. Exponential Growth of LBL Films with Incorporated Inorganic Sheets. *Nano Lett.* **2008**, *8*, 1762−1770.
(44) Xu, L.; Ankner, J. F.; Sukhishvili, S. A. Steric Effects in Ionic Pairing and Polyelectrolyte Interdiffusion within Multilayered Films: A Neutron Reflectometry Study. *Macromolecules* **2011**, *44*, 6518−6524.

DOI: 10.1021/acsami.5b03179
ACS Appl. Mater. Interfaces 2015, 7, 13597−13603